DEEJ (2023) 12 (8) 1-14

University of Kashan

Desert Ecosystem Engineering Journal

Journal homepage: http://deej.kashanu.ac.ir

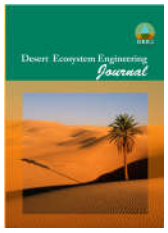

# Evaluating the Effects of Vegetation Types on Surface Temperature and Surface Moisture Using Satellite-Based Indices

Setareh Moazzam[1], Mohammad Hossein Mokhtari[2]*, Asghar Mosleh Arani[3], Hamid Reza Azimzadeh[2], Gholamhossein Moradi[2], Fatemeh Boomeh[4]

Received: 05/01/2021 Accepted: 22/01/2023

**Abstract**

As evaluating the influence of vegetation types on soil surface moisture (SSM) and soil surface temperature (LST) is crucially important, especially in semi-arid regions, this study set out to do so using remote sensing data. To this end, the vegetation types together with their extent of coverage in the study area were determined via the physiognomic-floristic method. In this regard, taking the results of field observations into account, eight types of vegetation were recognized and the zonation was performed.

Moreover, LST and SSM were calculated using the data collected from Landsat 8 on May 24 and July 27, 2017, followed by the evaluation of SST and SSM measurements by comparing them to the measurements made based on field studies ($R^2$>0.6). Then, at each vegetation zone, the influence of vegetation types on the SSM and the SST was statistically analyzed.

Duncan's statistical test showed significant differences between the mean temperature (α=0.05) in all vegetation types, except for the *Artemisia aucheri-Pistacia atlantica* and *Artemisia sieberi–Ebenus stellata-Cousinia desertii* in the first period of the study and the *Cynodon dactylon* and *Amygdalus scoparia-Pistacia atlantica* in the second period of the investigation.

However, SSM differences were found to be insignificant between *Artemisia sieberi–Amygdalus scoparia* and *Amygdalus scoparia* vegetation types in the first period of the study, and between *Amygdalus scoparia* and *Cynodon dactylon* vegetation types in the second period of the study. On the other hand, most vegetation types exerted a considerably varying influence on SST and SSM. Nonetheless, in both study periods, the temperature and moisture variations did not follow the same patterns in different vegetation types.

**Keywords:** Vegetation Type, Soil Surface Temperature, Soil Surface Moisture, Natural forest, Remote sensing.

1. MSc in Environmental Science, Faculty of Natural Resources, Yazd University, Yazd, Iran
2. Associate Professor, Faculty of Natural Resources, Yazd University, Yazd, Iran; Corresponding Author: mh.mokhtari@yazd.ac.ir
3. Professor, Faculty of Natural Resources, Yazd University, Yazd, Iran
4. PhD student, Faculty of Natural Resources, Yazd University, Yazd, Iran
DOI: 10.22052/JDEE.2023.240421.1072

## 1. Introduction

Bagh Shadi forest, the largest natural forest in Yazd province located in the southernmost area of Yazd province, Khatam city, Iran. The Bagh Shadi forest is considered unique in terms of type, composition, and size in the province. However, due to the sensitive and fragile ecological conditions of the region and the unrelenting pressure from livestock owners, irreparable damage has been inflicted on the valuable species of the region.

Fire is usually regarded as an ecological factor in forest destruction and restoration, the significance of which varies in different regions in terms of the consequences it brings about, considering the fact that the intensity of fire depends on the local climatic conditions of the area where it occurs (Certini, 2005).

Soil can be defined as a set of organic and inorganic materials on the surface of the earth, providing the grounds for plant growth. Soil temperature (ST) is known as a significant variable in hydrological (Pradhan et al. 2019), agro-meteorological (Aggarwal et al. 2006; Waring and Running 2007), and climate studies (Donglian and Pinker 2004; Pablos et al. 2016), whose correlation with crop growth has been proved in previous studies (Hillel 2005; Sabri et al. 2018; Waring and Running 2007).

Moreover, evaluating the ST's seasonal and daily variations, which may result from changes in radiant energy, gains more importance in studying the extent and the direction of the physical processes (Hillel 2005; Yolcubal et al. 2004), including alteration and its mineralization (Doran and Smith 1987). On the other hand, soil surface temperature (SST) depends on atmospheric humidity, surface emissivity, and the amount of energy released to the earth's surface (Vanhellemont 2020).

However, ST fluctuations vary over time and space, occurring primarily through the soil surface in response to the changes in the radiant, thermal, and latent energy exchange processes (Maiti and Kumar 2016). Furthermore, due to the soil's high thermal inertia, temperature fluctuations in the surface of the ground diminish with an increase in the depth of the ground (Florides et al. 2005; Sriboon et al. 2017).

The SST also affects the soil's water content, its conductivity, and its availability for plants (Onwuka 2018). Therefore, the extent of daily changes in SST is an important indicator of the soil's moisture (Wan et al. 2004). On the other hand, the interrelationship between SM and SST depends on the energy balance components. In other words, from among the componential elements of water balance, evaporation is closely associated with the latent heat of vaporization, making the estimation of SST of crucial importance in examining soil moisture. Therefore, estimating SST bears a great significance in retrieving the SM retrieval. Moreover, water and heat transport acts interactively in cases where temperature gradients affect moisture potential and the movement of liquid and vapor in soil (McInnes 2002).

Although the above-mentioned atmospheric-related physical parameters are influential in ST and SM variations, it is the soil coverage, including vegetation and plant residue, that regulates the SST (Xiong et al. 2019). On the other hand, the variations of the SM's content can be attributed to plant canopy features (Sriboon et al. 2017), which, together with the canopy's shadow, reduce soil exposure to solar radiation, making variations in SM and moisture content. Therefore, the higher the percentage of vegetation density, the lower the heat transferred to the soil would be due to the higher expected absorption of plants.

Moreover, vegetation greatly contributes to adjusting atmospheric humidity, moderating

wind velocity near the soil surface (McIvor et al. 2015), accommodating edaphic conditions (Tracey 1969), and controlling erosion (Blanco-Canqui and Lal 2008; Wu et al. 2019), especially in forested areas.

Meteorological stations routinely measure ST and SM using different types of sensors. Nevertheless, the generalization of point-based measurements of these spatial and temporal variables is impractical, requiring an appropriate statistical method, which is by no means error-free. Currently, satellite imagery is used to extract and measure land surface temperatures (LST) and SM, where the waves backscattered from the Earth's surface are measured in visible and infrared wave bands.

Possessing various spatial and temporal resolutions, including METEOSAT meteorological sensors, NOAA/AVHRR, and Terra/MODIS, satellite data have so far been used to estimate LST and SSM through space. However, compared to the available satellite data, the relatively high spectral and radiometric resolution of the Landsat 8 data set can, with its moderate resolution, be greatly exploited to help estimate LST and SSM values. Accordingly, assuming the dissimilarity of LST/SSM in different vegetation types, this study examined the relationship between vegetation types, soil temperature, and soil moisture using remote sensing data obtained from different vegetation types in Bagh-e-Shadi protected forest area in Iran.

Located in the southernmost area of Yazd province in Khatam city, Bagh-e-Shadi is the largest natural forest in Yazd. It is also considered as a unique forest in terms of type, composition, plant, and animal genetic resources. However, due to the sensitive and fragile ecological conditions of the region and the unrelenting pressure from livestock owners, irreparable damage has been inflicted on the valuable species of the region. Furthermore, the area has frequently been affected by fire due to drought, unsafe human activity, and the sensitiveness of plant species.

Fire is usually considered as an ecological factor in forest destruction and restoration. Investigating the possibility of monitoring the humidity and thermal condition of the earth's surface can play an important role in managing the protection of the valuable area. Therefore, this study evaluated the capability of satellite-based data in detecting soil moisture and temperature and their variations in various vegetation types.

## 2. Materials and methods

### 2.1. Description of the study area

The study area (fig 2) is a protected forest, located in the southern part of the Yazd province, Iran (Figure 2). Covering 11665 hectares, the area lies between the latitudes of 29◦ 42' 50" and 29◦ 50' 41" west, and the longitude of 54◦14′ 00″ and' 54◦ 42' 50" north, with its altitude varying from 1840 m to 2664 m above the sea level, which generally follows a decreasing trend from west to east. Moreover, the area’s average annual precipitation (mostly occurring during the winter) and temperature rates are roughly 285.2 mm and 13.3°C, respectively. Therefore, according to the De-Marton climate classification method, the study area is known as a semi-arid region.

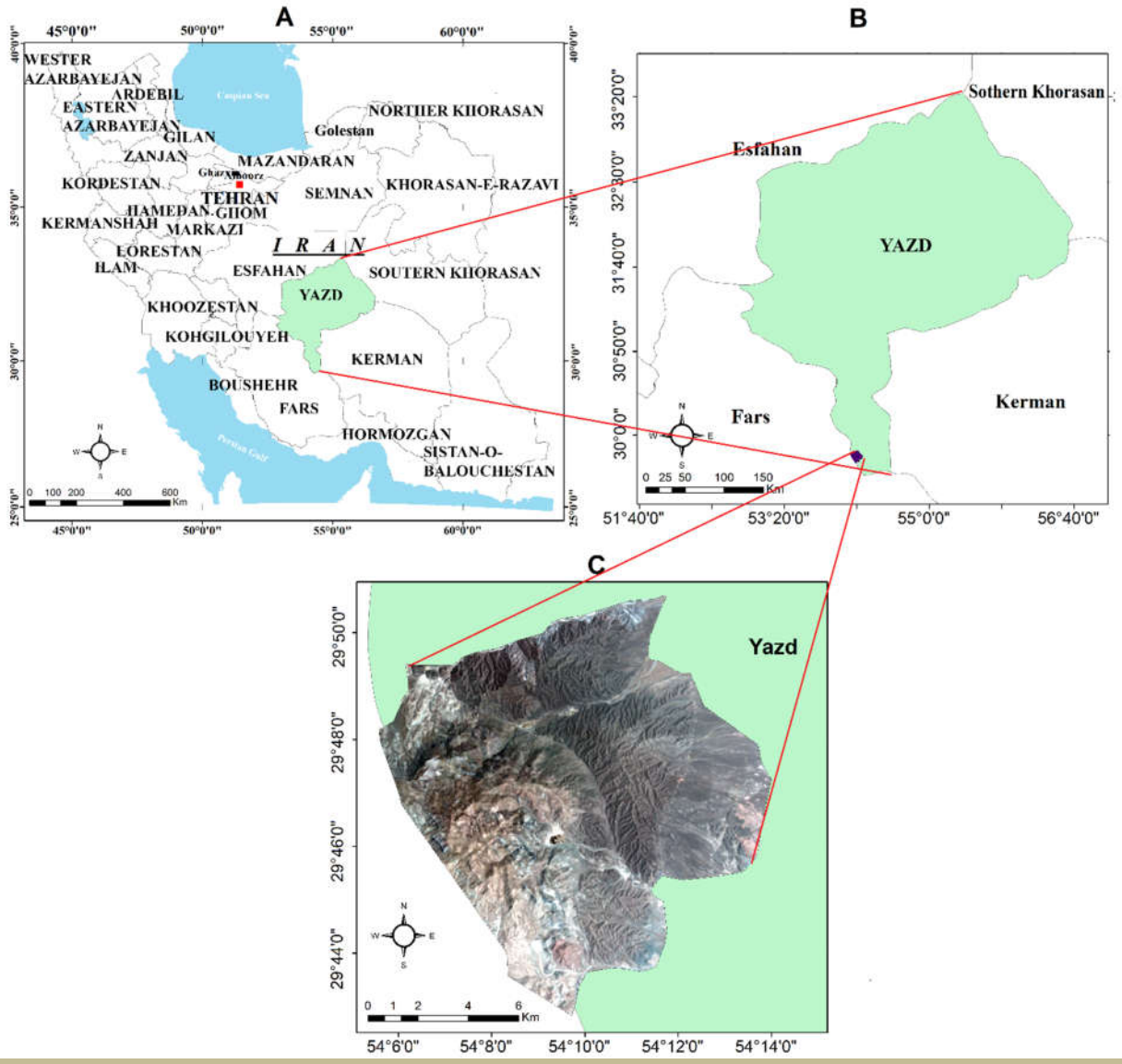


**Figure (1): The study area. A) Location of the study area in Iran, B) An overview of the study area in Yazd province, C) The Landsat 8 natural RGB image of the study area**

## 2.2. The Data used in the study

The data used in this study comprises satellite and field studies data. The satellite data consist of two LANDSAT 8 scenes (data of OLI and TIRS) taken on May 24 and July 27, 2017, which were preprocessed through the stages described below.

## 2.3. Pre-processing and processing the Satellite data

To estimate the LST and SSM values via satellite data, two cloud-free Landsat 8 scenes (path/row of 162/39), taken on May 24 and July 27, 2017, were downloaded from the website of the U.S Geological Survey (USGS) (https://www.usgs.gov). The data were then calibrated to the convertible original pixel value on the top of atmosphere reflectance (-) for the reflective bands, and to the radiance value ($W.m^{-2}.sr^{-1}$) for the emissive bands (Tasumi et al. 2005).

Moreover, the log-residual method was applied to remove the atmospheric effects. The method is designed to remove solar irradiance, atmospheric transmittance, instrument gain, and topographic and albedo effects from radiance data using merely in-scene statistics to perform

calibration (Green 1985). The geometric correction was also controlled by comparing the well-distributed 20-point coordinates on the image to the ground control points and calculating RMSE (Root Mean Square Error) value to be less than half of the original pixel's size.

On the other hand, the LST was calculated based on the Landsat 8 thermal bands, following the split-windows algorithm presented by Jiménez-Muñoz et al. (2014) as follows:

$$T_s = T_i + C_1(T_i - T_j) + C_2(T_i - T_j)^2 + C_0 + (C_3 + C_4 w)(1 - \varepsilon) + (C_5 + C_6\omega)\Delta\varepsilon$$

where $T_i$ and $T_j$ stand for the at-sensor brightness temperature at the SW bands i and j (k), ε represents the mean emissivity, where $\varepsilon = 0.5\ (\varepsilon_i + \varepsilon_j)$; Δε shows the emissivity difference, where $\Delta\varepsilon = (\varepsilon_i - \varepsilon_j)$; ω indicated the total atmospheric water vapor content ($g.cm^{-2}$), and $c_0$, $c_1$, $c_2$, $c_3$, $c_4$, $c_5$, and $c_6$ represent the split-window coefficients equaling -0.268, 1.378, 0.183, 54.30, -2.238, -129.20, and 16.40, respectively (Markham and Barker 1986).

Furthermore, the Land Surface Emissivity (LSE) was calculated via the following equation:

$$\mathrm{LSE} = \mathrm{ES} * (1 - \mathrm{FVC}) + \mathrm{E\,V} * \mathrm{FVC}$$

where ES stands for the soil emissivity, EV represents the vegetation emissivity (whose values for bands 10 and 11 are presented in table 2), and FVC is the fractional vegetation calculated through the following equation:

$$\mathrm{FVC} = (\mathrm{NDVI} - \mathrm{NDVIsoil}) / (\mathrm{NDVIvegetation} - \mathrm{NDVIsoil})$$

where NDVI stands for the Normalized Difference Vegetation Index, which is calculated by the red (band 4) and near-infrared (Nir, Band 5) bands of Landsat 8 images as follows:

$$NDVI = \frac{Nir - Red}{Nir + Red}$$

**Table (1): Soil and vegetation emissivity values for bands 10 and 11 of Landsat 8**

| Emissivity | Band 10 | Band 11 |
|---|---|---|
| $\varepsilon_S$ | 0.971 | 0.977 |
| $\varepsilon_V$ | 0.987 | 0.989 |

The spatial relationships between land surface temperature and vegetation index, proposed for the first time by Goward et al. (2002), were successfully applied to estimate the soil's moisture content. Depending on vegetation and soil moisture, the LST, together with the vegetation index, creates a triangular space characterized by two physical bounds, i.e. wet and dry edges (Sandholt et al. 2002). The edges mentioned in the figure show the range of two situations, i.e., soil moisture and evapotranspiration (figure 3).

Several indices can be calculated based on the triangular or trapezoidal space mentioned above. In this regard, Soil Wetness Index (SWI) is a highly important index that can successfully be used to model soil moisture conditions. The index is calculated through the following equation proposed by Mallick et al. (2009):

$$SWI = \frac{T_{s_{max}} - T_{s_i}}{T_{s_{max}} - T_{s_{min}}}$$

where $T_{si}$ stands for the observed surface temperature at a given pixel, $T_{s_{min}}$ represents the minimum surface temperature and defines the wet edge, and $T_{s_{max}}$ shows the maximum land surface temperature for $i^{th}$ NDVI, which is calculated via an empirical linear model as follows:

$$T_{s_{max}} = a + bNDVIi$$

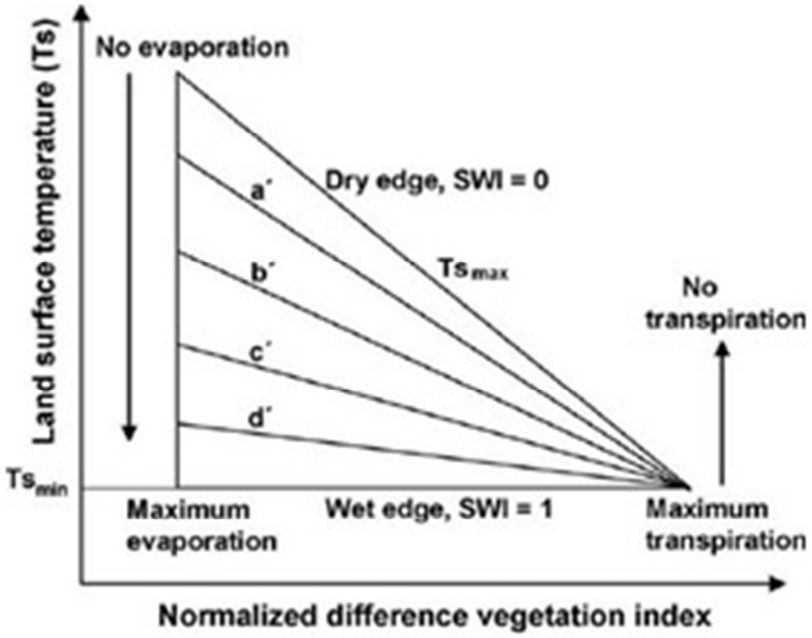


**Figure (2): The conceptual diagram of the surface temperature–vegetation index in a triangular space (Mallick et al. 2009)**

### 2.4. The data collected from field studies

Vegetation types were studied in different parts of the study region using field observation. Then, the dominant vegetation types and the extent of their coverage were determined through the physiognomic-floristic method (Gilbertson et al. 1985). Accordingly, with the help of physiographic maps at the 1: 25000 scale, the initial classification of vegetation types was performed based on the physiognomy and the main constituent species following field visits. Then, the percentage of vegetation coverage and its relative density were determined based on the samples taken from the dominant vegetation types. The sampling plot size was designated as 20 m × 20 m (400 $m^2$) and 10m × 10m (100 $m^2$) for trees/shrubs and herbal vegetation species, respectively.

In each sampling plot, vegetation features were specified, including vegetation types, main species, concomitant species, distributing dominant species, percentage of vegetation coverage, and relative vegetation density. Moreover, the floristic list was provided based on the collected plant specimens and the photos taken of different species observed in the region. Then, the plant species were identified using the authoritative scientific sources for botanical plants, the vegetative forms and scientific names of which were presented based on the Raunkiær system.

On the other hand, field-based LST (LST_G) was measured through a portable contact-free infrared thermometer (Scan Temp 330), which can measure the temperature rates ranging from -50°C to 330°C. Furthermore, Cochran's formula in which the size of the community is unknown was applied to determine the sample size using the following equation (as proposed by Cochran (2007)):

$$n = \frac{Z^2 pq}{d^2}$$

eq. 1

In the above equation, n represents the sample size, $Z^2$ stands for the abscissa of the normal curve that cuts off an area α at the tails, d is the degree of precision, p shows the proportion of the population with its characteristic p = 0.5 (assuming maximum heterogeneity, and q represents 1-p. t value, which can be found in the statistical tables.

The variance of samples was primarily evaluated by initial sampling inside the twelve plots distributed over the study area. Then, based on the values of the initial sample's standard

deviation, α value (0.29) and Z value (1.06) were calculated for the sample size (n=26).

The temperature rates were measured by averaging continuous measurements at a radius of 80 meters around the selected random points. Moreover, soil sampling was performed concerning the soil's moisture measurement (SSM_G). Moisture sampling at each point consisted of four sub-samples randomly located 70-80 meters away from each other around the sample point. Each sample was then mixed to obtain an identical sample.

To carry out the sampling, two days were individually selected from spring and summer, which coincided with the Landsat 8 overpass times and dates. In this regard, a total number of fifty-two samples were collected from different vegetation types. On the other hand, the samples' moisture content was measured by subtracting pre- and post-drying soil weight at 105 C° in the oven for 48 hours, whose values were then presented in terms of the soil's dry mass percentage.

Furthermore, the relationship between the satellite-based SSM (SSM_S) and LST (LST_S) was evaluated in different vegetation types. Pearson's statistical test was also conducted to evaluate the significance of the correlation between the field-studies-based measurement and the satellite estimates over various vegetation types. Finally, the mean comparison of the variables was conducted based on Duncan's statistical test to show whether or not the differences between the variables and vegetation types were significant.

## 3. Results

Based on the data collected from field studies, eight types of vegetation were identified. Table 1 shows the summary of the results obtained from investigating vegetation in the study area.

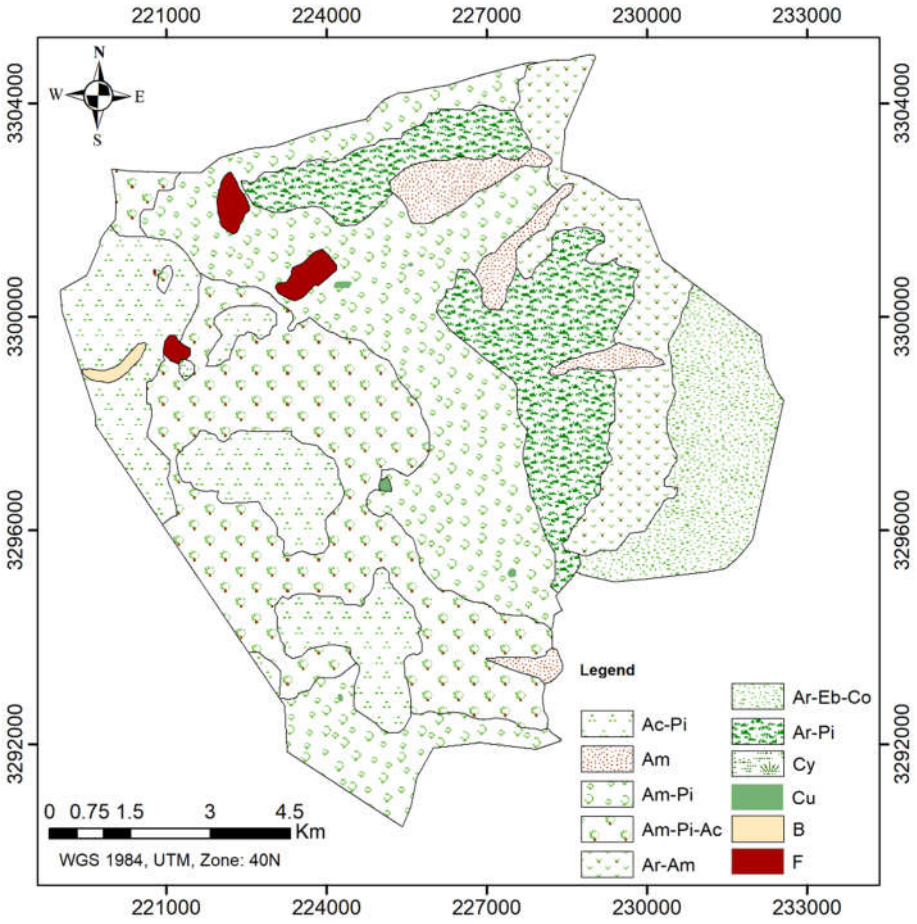


**Figure (3): The map of vegetation types**

**Table (2): Vegetation types of the study area**

| Vegetation Type | Symbol | Area (ha) | Elevation above sea level (m) |
|---|---|---|---|
| *Amygdalus scoparia-Pistacia atlantica* | Am-Pi | 3338 | 1900-2300 |
| *Acer monspessulanum-Pistacia atlantica* | Ac-Pi | 1655 | 2100-2662 |
| *Amygdalus spp. -Pistacia atlantica-Acer monspessulanum* | Am-Pi-Ac | 2621 | 2000-2500 |
| *Artemisia aucheri-Pistacia atlantica* | Ar-Pi | 1538 | 1950-2150 |
| *Amygdalus scoparia* | Am | 401 | 1900-2050 |
| *Artemisia sieberi –Amygdalus scoparia* | Ar-Am | 1010 | 1850-2050 |
| *Artemisia sieberi –Ebenus stellata-Cousinia desertii* | Ar-Eb-Co | 990 | 1840-1920 |
| *Cynodon dactylon* | Cy | 8 | 2390 |
| *Burned forest* | F | 0.6 | 2060-2475 |
| *Bare Land* | B | 29 | 2357--2577 |
| *Cultivated land* | Cu | 7.6 | 2083-2099 |

Table 3 shows the descriptive statistics of the moisture and temperature rates obtained from the field- and satellite-based measurements carried out in the sample points throughout two different periods investigated in this empirical study. Accordingly, on May 24, 2017, the minimum, maximum, and average temperature rates of the soil were 47 □, 54.5 □, and 51.01 □, respectively. The rates increased on July 27, 2017, when the second investigation was conducted, with the standard deviation getting slightly decreased.

Similar results were found for soil moisture, with the minimum, maximum, and average rates of soil moisture being 15%, 48%, and 32% on the first date of investigation, respectively, which were slightly higher than the values recorded for the second period. As shown in table 3, temperature and moisture followed a reversal trend toward one another in the two periods mentioned. However, the results of the field studies-based LST/SSM were consistent with those found by the satellite-based estimates, following a similar trend. In general, figure 4 indicates a negative correlation between soil moisture and LST.

**Table (3): Descriptive statistics of field-studies-based and satellite-derived soil moisture/temperature at sample points**

| Date | Method | Minimum | Maximum | Mean | Std. Deviation |
|---|---|---|---|---|---|
| May 24, 2017 | LST_G | 47.10 | 54.60 | 51.01 | 1.82 |
| | LST_S | 45.50 | 51.00 | 48.60 | 1.41 |
| | SSM_G | 0.15 | 0.48 | 0.32 | 0.09 |
| | SSM_S | 0.24 | 0.50 | 0.36 | 0.07 |
| July 27, 2017 | LST_G | 51.30 | 57.90 | 54.68 | 1.69 |
| | LST_S | 50.40 | 54.10 | 52.12 | 1.09 |
| | SSM_G | 0.06 | 0.27 | 0.15 | 0.05 |
| | SSM_S | 0.07 | 0.26 | 0.18 | 0.06 |

LST values are reported in degree Celsius (°C) units and the SSM values are presented in a range from 0 to 1

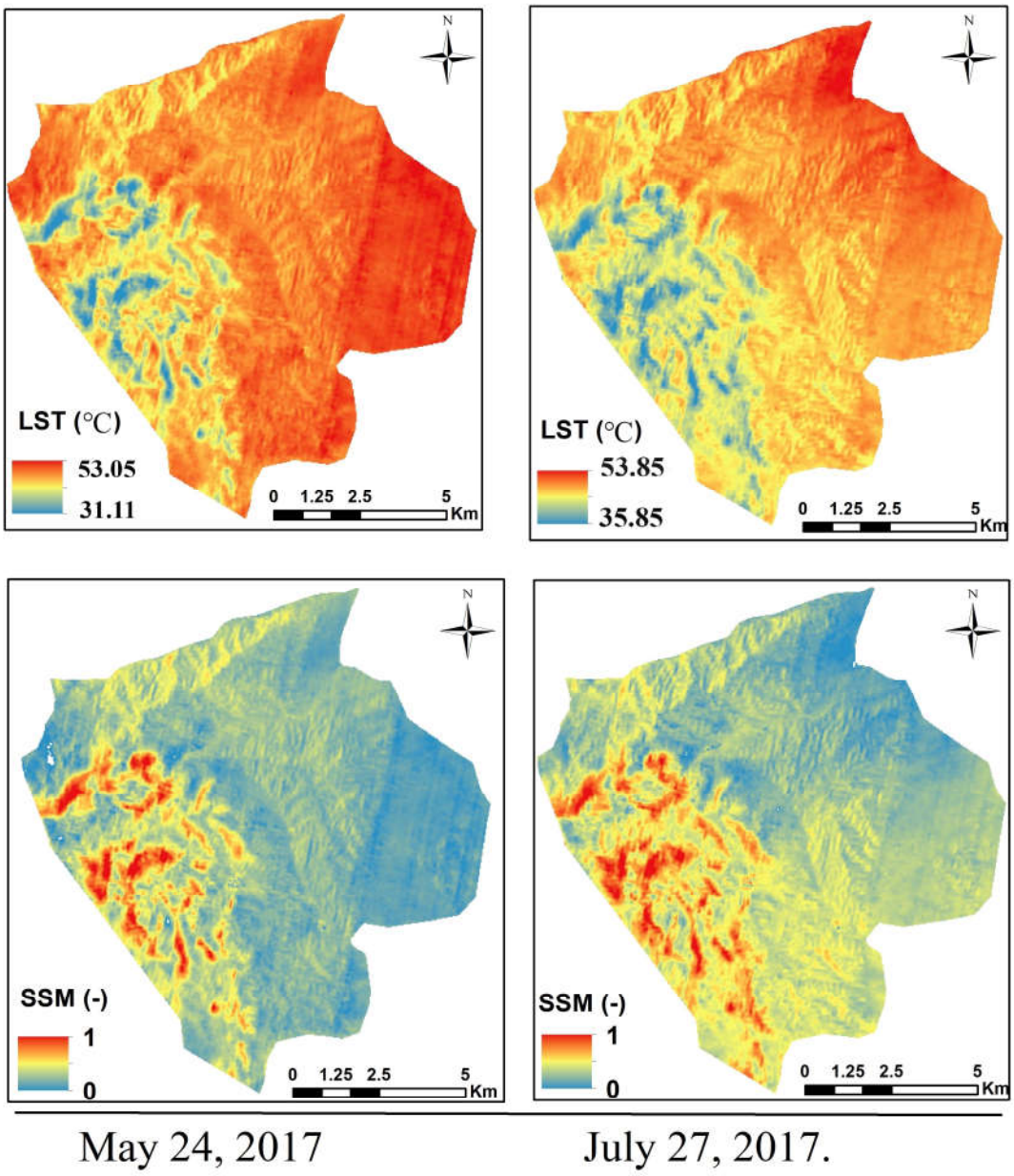


**Figure (4): LST and SSM_S maps generated by the surface temperature–vegetation index in a triangular space on May 24 and July 27, 2017**

Figures 5A and 6A show the scatter plots of LST_G and LST_S developed for the two periods investigated in this study. Accordingly, the linearity of the relationship between the two variables under investigation was obvious (the $R^2$ values of LST_G and LST_S being 0.702 and 0.63 on May 24 and July 27, 2017, respectively). Similarly, a linear relationship was evidently found between SSM_G and SSM_S, with their correlation coefficients being 0.765 and 0.818, respectively (as presented in Figure 5). Table 4 shows the results of Pearson's correlation tests concerning the LST/SSM obtained from the direct field studies and satellite estimates at the 0.01 confidence level (2-tailed). Accordingly, the correlations between all variables were proved to be significant. Generally, it was found that soil moisture and temperature were negatively correlated with each other. Moreover, the highest correlation value (-0.889) was found in the SSM_S and LST_S pairs, and the lowest correlation was observed between the SSM_G and LST_G (-0.603).

**Table (4): Correlation matrix of field-studies-based measurement and satellite-based estimates**

| Date | Variable | LST_G | LST_S | SSM_G | SSM_S |
|---|---|---|---|---|---|
| May 24, 2017 | LST_G | 1 | | | |
| | LST_S | 0.838 | 1 | | |
| | SSM_G | -0.603 | -0.866 | 1 | |
| | SSM_S | -0.841 | -0.998 | 0.874** | 1 |
| July 27, 2017 | LST_G | 1 | | | |
| | LST_S | 0.794 | 1 | | |
| | SSM_G | -0.731 | -0.906 | 1 | |
| | SSM_S | -0.794 | -0.998 | 0.904 | 1 |

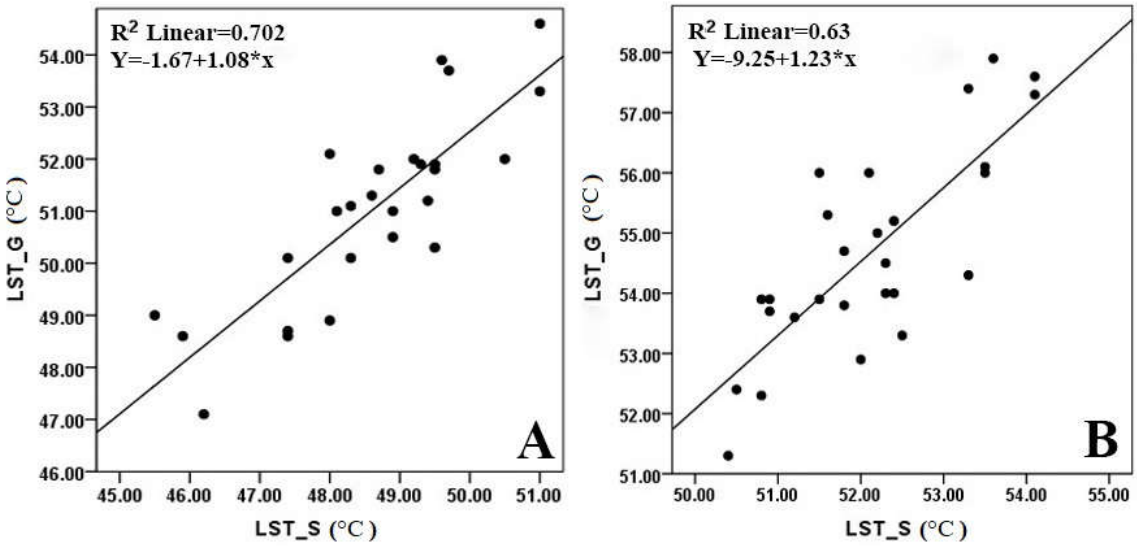


**Figure (5): Scatter plot of LST_G and LST_S on May 24, 2017 (A) and on July 27, 2017 (B)**

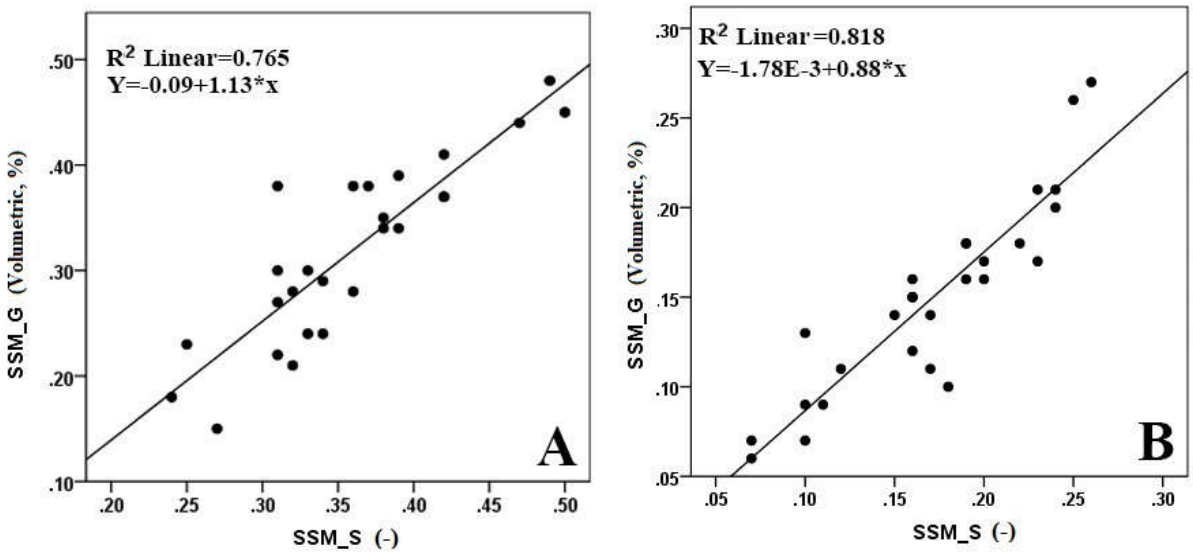


**Figure (6): Scatter plot of SSM_G and SSM_S on May 24, 2017 (A) and on July 27, 2017 (B)**

According to the above-mentioned results and due to the existence of a significant correlation between satellite-based estimates and field studies, the relationship between the vegetation types and the satellite-based variables, that is the SSM_S/LST_S, was

investigated. On the other hand, a one-way analysis of variances (ANOVA) test was performed to find out whether or not the vegetation types exerted any influence on the moisture content and the surface temperature of the soil. To this end, first, the normality and the homogeneity of the variables' variance, i.e., the main assumptions of using ANOVA, were verified. In this regard, the results of the Kolmogorov–Smirnov test and Levene statistics suggested that the variables were normally distributed. However, the equality of the variables' variance in different vegetation types was rejected.

Tables 5 and 6 show the results of the variables' mean comparison made based on Duncan's statistical test, indicating a significant difference between the average temperature rates ($\alpha$=0.05) in all vegetation types, except for AR_PI and AR_EB_CO on the first period and the CY and AM_PI on the second period investigated in this study. Furthermore, the SSM_S differences were found to be insignificant between AR_AM and AM vegetation types in the first period and between AM and CY vegetation types in the second period under investigation (Tables 7 and 8).

**Table (5): Analysis of LST_S variance in different vegetation types on May 24, 2017**

| Veg. Type | 1 | 2 | 3 | 4 | 5 | 6 | 7 |
|---|---|---|---|---|---|---|---|
| AC_PI | 315.82 | | | | | | |
| AM_PI_AC | | 316.64 | | | | | |
| CY | | | 318.32 | | | | |
| AM_PI | | | | 319.06 | | | |
| AR_PI | | | | | 320.56 | | |
| AR_EB_CO | | | | | 320.75 | | |
| AM | | | | | | 321.30 | |
| AR_AM | | | | | | | 322.07 |

**Table (6): Analysis of LST_S variance in different vegetation types on July 27, 2017**

| Veg. Type | 1 | 2 | 3 | 4 | 5 | 6 | 7 |
|---|---|---|---|---|---|---|---|
| AC_PI | 320.88 | | | | | | |
| AM_PI_AC | | 321.73 | | | | | |
| CY | | | 323.24 | | | | |
| AM_PI | | | 323.44 | | | | |
| AR_PI | | | | 324.00 | | | |
| AM | | | | | 324.36 | | |
| AR_AM | | | | | | 325.34 | |
| AR_EB_CO | | | | | | | 326.11 |

**Table (7): Analysis of SSM_S variance in different vegetation types on May 24, 2017**

| Veg. Type | 1 | 2 | 3 | 4 | 5 | 6 | 7 |
|---|---|---|---|---|---|---|---|
| AR_AM | 0.163 | | | | | | |
| AM | 0.172 | | | | | | |
| AR_PI | | 0.207 | | | | | |
| AR_EB_CO | | | 0.235 | | | | |
| CY | | | | 0.258 | | | |
| AM_PI | | | | | 0.27 | | |
| AM_PI_AC | | | | | | 0.372 | |
| AC_PI | | | | | | | 0.413 |

**Table 8: Analysis of SSM_S variance in different vegetation types on July 27, 2017**

| Veg. Type | 1 | 2 | 3 | 4 | 5 | 6 | 7 |
|---|---|---|---|---|---|---|---|
| AR_EB_CO | 0.0995 | | | | | | |
| AR_AM | | 0.1347 | | | | | |
| AM | | | 0.1736 | | | | |
| CY | | | 0.1799 | | | | |
| AR_PI | | | | 0.1931 | | | |
| AM_PI | | | | | 0.2095 | | |
| AM_PI_AC | | | | | | 0.2854 | |
| AC_PI | | | | | | | 0.3322 |

## 4. Discussion

The comparison of the results shown in Tables 5 and 6 indicated that, apart from the types found in the last three rows, the arrangement of all vegetation types was the same in terms of average temperature in both periods of the study. However, compared to the first period, the surface average temperature was generally higher during the second period in the areas covered with different vegetation types. The higher temperature rate was well expected for hot months when the study continued for the second period.

Nonetheless, the moisture conditions of different vegetation types did not follow the same trend in the two periods of the study as the temperature conditions did. As can be seen in Tables 7 and 8, the first five vegetation types on the top of the tables were significantly different in terms of the soil's moisture index. On the other hand, just the same as the surface temperature, the surface moisture index decreased more greatly in all vegetation types during the second period than it did throughout the first one.

It is worth mentioning that the moisture index is calculated by combining the temperature and the vegetation indices. Therefore, varying from the first period to the second one, the moisture variations found in different vegetation types could somehow be attributed to the ratio of the plant combinations observed in different plant types and the variations found in their coverage at the end of the growing season.

The shadow of trees decreases the surface temperature, occurring specifically when grass cover, such as CY, degenerates earlier than shrubs and trees do during the growing season, with the moisture variations being more drastic in areas covered by grass. In other words, due to their extended roots, the grass types (CY) are affected by water deficit-induced stresses earlier than the shrubs and trees, especially when the weather begins to become hot, indicating the differences in moisture variations among the vegetation types studied during the second period.

It should be noted that the variations found in surface moisture and temperature could also be affected by other factors, including the physiographic features of the earth's surface.

## Conclusion

This study sought to investigate the influence of different vegetation types on surface temperature and moisture (that is, two important ecological parameters) in a protected area with natural vegetation. According to the data obtained from the field observations, it was found that the satellite-based data could be used with a relatively low rate of errors to estimate the temperature and the moisture content of the soil, which are considered as two important environmental parameters.

Therefore, it could be concluded that various vegetation types may affect the surface temperature of an area differently. Similarly, as the investigation of the surface moisture variations obtained from the SWI index showed, in most cases different rates were recorded for the average moisture of different vegetation types. In other words, different vegetation types affect the variations of the soil's surface temperature and moisture in a distinct way. However, the influence may vary due to variations in vegetation types' growth periods or variations in their greenness.

On the other hand, the biophysical characteristics and spectral reflectance's can

significantly be different over cold and warm seasons (Guo et al. 2000; He et al. 2020). In addition, the physical properties and the dried remains of these vegetation types reduce the energy absorption and moderate the surface temperature. Therefore, as these factors could play a significant role in determining the natural habitat of different vegetation types, their influence is embedded in the characteristics of some given plants.

Natural growth in a certain geographical area may depend on some specific factors. However, as the results obtained from two periods of investigation showed, unchanging factors, such as the environment, could not be regarded as mere determinants of temperature and moisture variations. Rather, the type of plants and the extent of their greenness might be considered as some other influential ecological parameters in this regard.

## References


1. Aggarwal PK, Kalra N, Chander S, Pathak H (2006) InfoCrop: A dynamic simulation model for the assessment of crop yields, losses due to pests, and environmental impact of agro-ecosystems in tropical environments. I. Model description Agricultural Systems 89:1-25 doi:https://doi.org/10.1016/j.agsy.2005.08.001
2. Blanco-Canqui H, Lal R (2008) Soil Erosion Under Forests. In: Principles of Soil Conservation and Management. Springer Netherlands, Dordrecht, pp 321-344. doi:10.1007/978-1-4020-8709-7_12
3. Certini G. Effects of fire on properties of forest soils: a review. Oecologia. (2005) Mar;143(1):1-10. doi: 10.1007/s00442-004-1788-8.
4. Cochran WG (2007) Sampling Techniques, 3Rd Edition. Wiley India Pvt. Limited,
5. Donglian S, Pinker RT (2004) Case study of soil moisture effect on land surface temperature retrieval IEEE Geoscience and Remote Sensing Letters 1:127-130 doi:10.1109/LGRS.2004.824749
6. Doran JW, Smith MS (1987) Organic matter management and utilization of soil and fertilizer nutrients. SSSA Special Publication, vol 19. Soil Science Society of America and American Society of Agronomy, Madison, WI. doi:10.2136/sssaspecpub19.frontmatter
7. Florides GA, Kalogirou SA, Florides GA (2005) Annual ground temperature measurements at various depths.
8. Gilbertson DD, Kent M, Pyatt FB (1985) Describing vegetation in the field — physiognomic methods. In: Practical Ecology for Geography and Biology: Survey, mapping and data analysis. Springer US, Boston, MA, pp 59-74. doi:10.1007/978-1-4684-1415-8_4
9. Goward SN, Xue Y, Czajkowski KP (2002) Evaluating land surface moisture conditions from the remotely sensed temperature/vegetation index measurements: An exploration with the simplified simple biosphere model Remote Sensing of Environment,79:225-242 doi:https://doi.org/10.1016/S0034-4257(01)00275-9
10. Green AA (1985) Analysis of aircraft spectrometer data with logarithmic residuals Proc Airborne Imaging Spectrometer Data Analysis Workshop 85:111-119
11. Guo X, Price KP, Stiles JM (2000) Biophysical and Spectral Characteristics of Cool- and Warm-Season Grasslands under Three Land Management Practices in Eastern Kansas Natural Resources Research 9:321-331 doi:10.1023/A:1011513527965
12. He Y, Yan H, Ma L, Zhang L, Qiu L, Yang S (2020) Spatiotemporal dynamics of the vegetation in Ningxia, China using MODIS imagery Frontiers of Earth Science 14:221-235 doi:10.1007/s11707-019-0767-7
13. Hillel D (2005) THERMAL PROPERTIES AND PROCESSES. In: Hillel D (ed) Encyclopedia of Soils in the Environment. Elsevier, Oxford, pp 156-163. doi:https://doi.org/10.1016/B0-12-348530-4/00523-3
14. Jiménez-Muñoz JC, Sobrino JA, Skoković D, Mattar C, Cristóbal J (2014) Land Surface Temperature Retrieval Methods From Landsat-8 Thermal Infrared Sensor Data IEEE Geoscience and Remote Sensing Letters 11:1840-1843 doi:10.1109/LGRS.2014.2312032
15. Maiti SK, Kumar A (2016) Chapter 2 - Energy Plantations, Medicinal and Aromatic Plants on Contaminated Soil. In: Prasad MNV (ed) Bioremediation and Bioeconomy. Elsevier, pp 29-47. doi:https://doi.org/10.1016/B978-0-12-802830-8.00002-2
16. Mallick K, Bhattacharya BK, Patel NK (2009) Estimating volumetric surface moisture content for cropped soils using a soil wetness index based on surface temperature and NDVI Agricultural and Forest Meteorology 149:1327-1342.

doi:https://doi.org/10.1016/j.agrformet.2009.03.004
17. Markham BL, Barker JL (1986) Landsat MSS and TM Post-Calibration Dynamic Rangers, Exoatmospheric Reflectance and At-Satellite Temperatures. EOSAT Landsat Tech. Notes, 3-8.
18. McInnes KJ (2002) Soil heat. In: Topp JHDaGC (ed) Methods of soil analysis. Madison, WI, pp 1183–1199.
19. McIvor A, Spencer T, Spalding M, Lacambra C, Möller I (2015) Chapter 14 - Mangroves, Tropical Cyclones, and Coastal Hazard Risk Reduction. In: Shroder JF, Ellis JT, Sherman DJ (eds) Coastal and Marine Hazards, Risks, and Disasters. Elsevier, Boston, pp 403-429. doi:https://doi.org/10.1016/B978-0-12-396483-0.00014-5
20. Onwuka B (2018) Effects of Soil Temperature on Some Soil Properties and Plant Growth Advances in Plants & Agriculture Research 8 doi:10.15406/apar.2018.08.00288
21. Pablos M, Martínez-Fernández J, Piles M, Sánchez N, Vall-llossera M, Camps A (2016) Multi-Temporal Evaluation of Soil Moisture and Land Surface Temperature Dynamics Using in Situ and Satellite Observations Remote Sensing 8:587
22. Pradhan NR, Downer CW, Marchenko S (2019) Catchment Hydrological Modeling with Soil Thermal Dynamics during Seasonal Freeze-Thaw Cycles Water 11:116
23. Sabri NSA, Zakaria Z, Mohamad SE, Jaafar AB, Hara H (2018) Importance of Soil Temperature for the Growth of Temperate Crops under a Tropical Climate and Functional Role of Soil Microbial Diversity Microbes Environ 33:144-150 doi:10.1264/jsme2.ME17181
24. Sandholt I, Rasmussen K, Andersen J (2002) A simple interpretation of the surface temperature/vegetation index space for assessment of surface moisture status Remote Sensing of Environment 79:213-224 doi:https://doi.org/10.1016/S0034-4257(01)00274-7
25. Sriboon W, Tuntiwaranuruk U, Sanoamuang N (2017) Hourly soil temperature and moisture content variations within a concrete pipe container for planting lime trees in Eastern Thailand Case Studies in Thermal Engineering 10:192-198. doi:https://doi.org/10.1016/j.csite.2017.06.005
26. Tasumi M, Trezza R, Allen RG, Wright JL (2005) Operational aspects of satellite-based energy balance models for irrigated crops in the semi-arid U.S Irrigation and Drainage Systems 19:355-376 doi:10.1007/s10795-005-8138-9
27. Tracey JG (1969) Edaphic Differentiation of some Forest Types in Eastern Australia: I. Soil Physical Factors Journal of Ecology 57:805-816 doi:10.2307/2258501
28. Vanhellemont Q (2020) Combined land surface emissivity and temperature estimation from Landsat 8 OLI and TIRS ISPRS Journal of Photogrammetry and Remote Sensing 166:390-402, doi:https://doi.org/10.1016/j.isprsjprs.2020.06.007
29. Wan Z, Wang P, Li X (2004) Using MODIS Land Surface Temperature and Normalized Difference Vegetation Index products for monitoring drought in the southern Great Plains, USA International Journal of Remote Sensing 25:61-72 doi:10.1080/0143116031000115328
30. Waring RH, Running SW (2007) CHAPTER 7 - Spatial Scaling Methods for Landscape and Regional Ecosystem Analysis. In: Waring RH, Running SW (eds) Forest Ecosystems (Third Edition). Academic Press, San Diego, pp 225-V. doi:https://doi.org/10.1016/B978-012370605-8.50014-1
31. Wu Z, Wang M, Zhang H, Du Z (2019) Vegetation and soil wind erosion dynamics of sandstorm control programs in the agro-pastoral transitional zone of northern China Frontiers of Earth Science 13:430-443 doi:10.1007/s11707-018-0715-y
32. Xiong Y, Peng F, Zou B (2019) Spatiotemporal influences of land use/cover changes on the heat island effect in rapid urbanization area Frontiers of Earth Science 13:614-627 doi:10.1007/s11707-018-0747-3
33. Yolcubal I, Brusseau ML, Artiola JF, Wierenga P, Wilson LG (2004) 12 - ENVIRONMENTAL PHYSICAL PROPERTIES AND PROCESSES. In: Artiola JF, Pepper IL, Brusseau ML (eds) Environmental Monitoring and Characterization. Academic Press, Burlington, pp 207-239. doi:https://doi.org/10.1016/B978-012064477-3/50014-X